Jordan Journal of Pharmaceutical Sciences, Volume 8, No. 2, 2015

Identification of Possible Glyoxalase II Inhibitors as Anticancer Agents by a Customized 3D Structure-Based Pharmacophore Model

Nizar A. Al-Shar'I [1]*, Mohammad Hassan [1], Qosay Al-Balas [1], Ammar Almaaytah[2]

[1] *Department of Medicinal Chemistry and Pharmacognosy, Faculty of Pharmacy, Jordan University of Science and Technology, Irbid, Jordan.*
[2] *Department of Pharmaceutical Technology, Faculty of Pharmacy, Jordan University of Science and Technology, Irbid, Jordan*

ABSTRACT

The glyoxalase system (which consists of glyoxalase-I and glyoxalase-II) is a ubiquitous metabolic pathway involved in cellular detoxification of the cytotoxic 2-oxoaldehydes. Tumour cells have high metabolic activity which results in increased cellular levels of such toxic metabolites. Therefore, tumour cells respond to this increase by increasing the activity of the detoxifying glyoxalase system which makes it a viable target for the development of anticancer drugs.
This work represents the first study that aims to find none-glutathione-based inhibitors of the glyoxalase-II enzyme as potential anticancer drugs based on computer aided drug design. In this study, a customized 3D structure-based pharmacophore model was generated which is a hybrid of three complementary 3D pharmacophores. Since glyoxalase-II is a binuclear zinc metalloenzyme, a customized Zn-binding pharmacophoric feature was added to the generated pharmacophore to aid the search for selective glyoxalase-II inhibitors through virtual screening of small-molecules databases. Retrieved hits were extensively filtered then docked into the binding site of the enzyme. In order to maximize the chances of finding potential inhibitors of glyoxalase-II, docked hits were rescored using different scoring functions and consensually scored. Ten of the top ranked hits were selected as potential glyoxalase-II inhibitors.

Keywords: Computer Aided Drug Design; Glyoxalase-II; Inhibitors; Anticancer.

1. INTRODUCTION

The glyoxalase system is a ubiquitous metabolic pathway present in cells' cytosol and other organelles, mainly the mitochondria. It is involved in cellular detoxification of the cytotoxic 2-oxoaldehydes, particularly methylglyoxal (MG), to the corresponding nontoxic 2-hydroxycarboxylic acid derivatives (lactic acid) using reduced glutathione (GSH) as a cofactor. The glyoxalase system consists of two distinct complementary enzymes; glyoxalase-I (Glo-I) and glyoxalase-II (Glo-II). Glo-I catalyses the isomerisation of hemithioacetal (formed spontaneously from methylglyoxal and GSH) into S-D-lactoylglutathione (SLG) that serves as a substrate for Glo-II which catalysis its hydrolysis to liberate the nontoxic D-lactic acid and regenerates GSH cofactor[1-3] (Figure 1).

* nashari@just.edu.jo
Received on 4/1/2015 and Accepted for Publication on 4/4/2015.

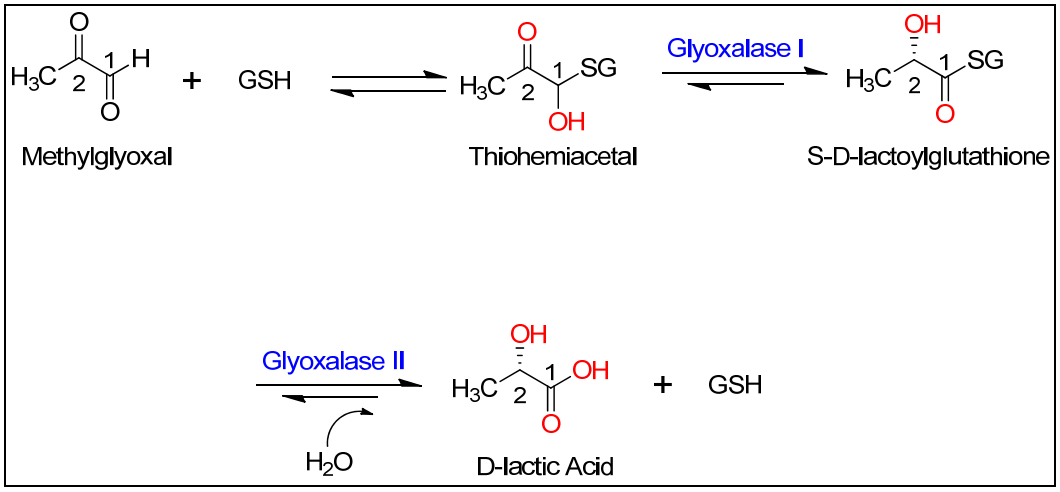

Figure 1: The glyoxalase system and the reactions it catalyses

MG is a toxic metabolite results mainly from non-enzymatic degradation of triosephosphates during glycolysis[4], and to a lesser extent from ketone body metabolism[5], threonine catabolism[6,7], and the degradation of glycated proteins[8]. MG cytotoxicity results from its ability to react with DNA, RNA, and proteins leading to an inhibition of their synthesis, stoppage of cell growth and apoptosis[9]. SLG also exhibits cytotoxic activity via inhibition of DNA synthesis. This cytotoxic effect was evident in many studies that investigated the anti-proliferative effect of SLG on human promyelocytic leukaemia HL60 cells. Interestingly, compared to tumour cells it showed no or low toxicity to differentiated and non-malignant proliferating tissues[10-13].

Highly proliferating cells, such as tumour cells, have high glycolytic activity which results in increased cellular levels of toxic MG and SLG metabolites. Therefore, tumour cells respond to this increase by increasing the activity of the detoxifying glyoxalase system to minimize the intracellular concentration of these metabolites. This was evident in breast carcinoma as reported by Rulli et al, where the activity levels of Glo-I and Glo-II were significantly higher in tumour (about 5.2 and 3.4-fold for Glo-I and Glo-II, respectively) compared to normal tissues[9]. Another study conducted by Mearini et al compared the activities and gene expression of the glyoxalase system enzymes in human superficial (SBC) or invasive bladder cancer (IBC) with the corresponding normal mucosa. This study showed that the activity of Glo-I was significantly increased in SBC, while it remained unchanged in IBC samples. Whereas, Glo-II showed a higher activity in both SBC and IBC samples compared to normal tissues[14].

Based on these findings, the glyoxalase system seems to be a viable target for the development of anticancer drugs that can inhibit either one or both enzymes in this system. Inhibition of Glo-I will result in the accumulation of MG, and that of Glo-II will result in the accumulation of the thioester (SLG) and depletion of the vital GSH; either way will result in cytotoxic effects on tumour cells. Attempts in this direction have already been established by developing inhibitors of Glo-I and Glo-II that are based mainly on glutathione derivatives (figure 2[15, 16] and table 1, respectively).

This work represents the first study that aims to find none-glutathione-based inhibitors of the Glo-II enzyme as potential anticancer drugs based on computer aided drug

design (CADD) techniques, namely: pharmacophore modelling, virtual screening and molecular docking.

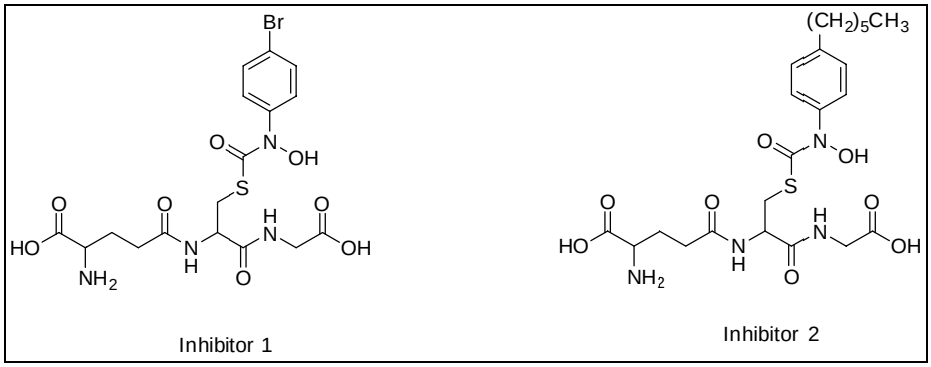

Figure 2: Examples of glutathione based inhibitors of Glo-I

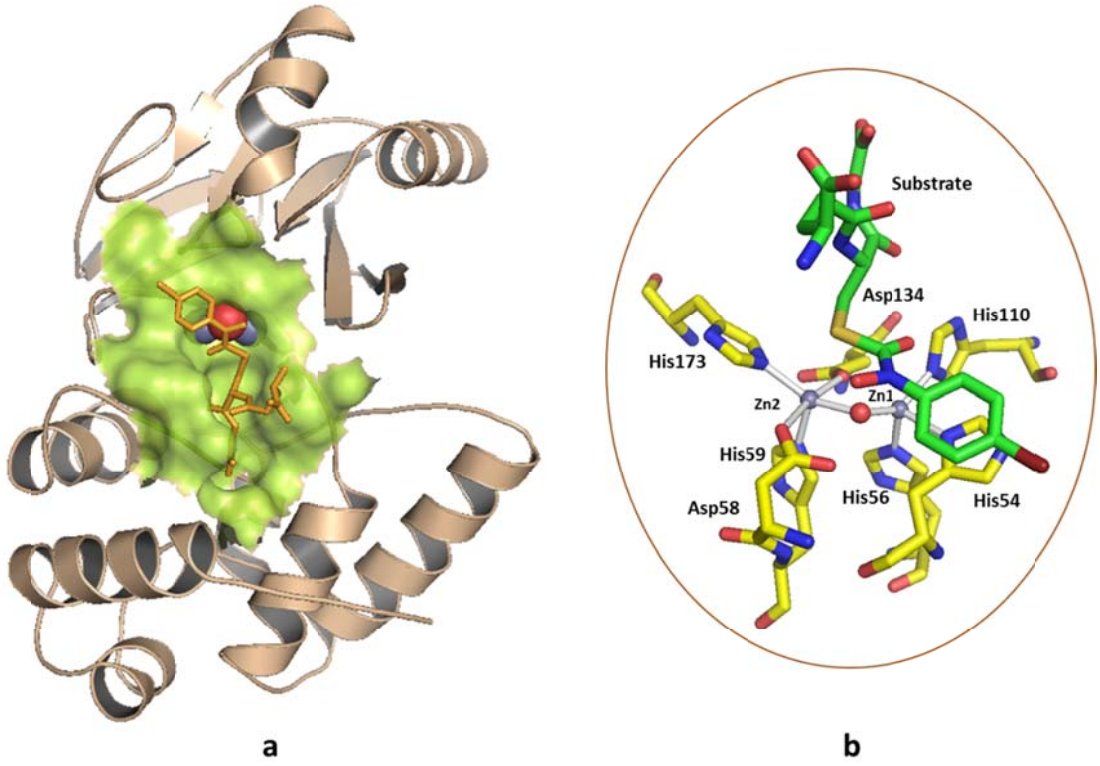

Figure 3: (a) The crystal structure of human Glo-II (pdb code 1QH5). The protein is shown in cartoon representation and coloured wheat, the binding site is shown in green surface and the Zn and $^{-}$OH ions are shown in purple and red spheres respectively. (b) A close-up view of the active site showing the amino acid residues involved in coordinating Zn ions along with the bridging water. The enzyme is in complex with the slow substrate GBP (green carbon skeleton)

Results and Discussion

1. Crystal structure of glyoxalase II

Glo-I is a mononuclear zinc enzyme[24], while Glo-II is a binuclear zinc metalloenzyme[25] However, Glo-II shows metal-binding flexibility with Fe and Mn, or Zn that have been characterized in different species[26]. Two X-ray crystal structures of human Glo-II have been determined and deposited in the protein data bank[27]; the first (PDB accession code 1QH3, resolution of 1.9Å) corresponds to Glo-II with cacodylate and acetate ions present in the active site; and the other (PDB accession code 1QH5, resolution of 1.45Å) corresponds to two Glo-II molecules in complex with glutathione and a substrate analogue, S-(N-hydroxy-N- bromophenylcarbamoyl) glutathione (GBP)[25].

In Glo-II, the active site contains two Zn ions that are bound to the protein by five amino acids namely: His54, His56, His110, Asp58, His59, Asp134 and His173. Furthermore, they are bridged by one oxygen from Asp134, and a hydroxide ion (OH^-) which is the nucleophilic species that attacks the substrate (figure 3). The proposed catalytic mechanism of Glo-II based on crystallographic, kinetic and computational studies involves the binding of the substrate followed by nucleophilic attack by the hydroxide ion; the role of the two Zn ions is to stabilise the negatively charged intermediates formed during the catalytic process[28, 29].

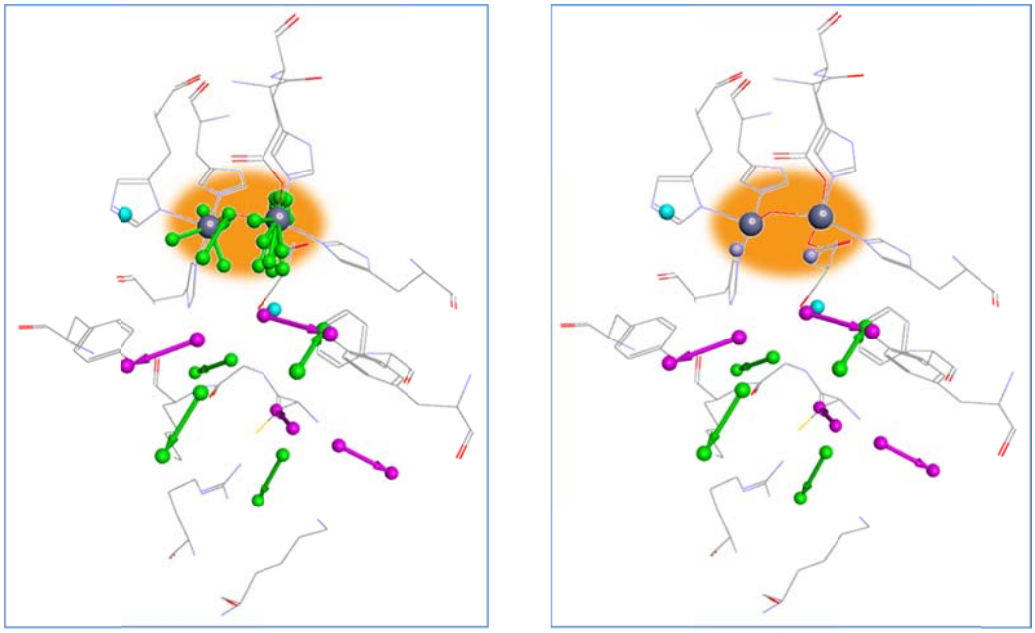

Figure 4: Clustered and edited features obtained from interaction generation protocol. Zn ions (large purple spheres) are treated by DS as HBD (which are complemented by HBA). (a) The Zn binding region is highlighted by the orange ellipsoid. Note the HBA features that map the Zn ions. (b) Replacing the HBA features that map Zn ions with a Zn-binder features (in purple). HBD are in magenta, HBA are in green, and the HY regions are in cyan.

2. Structure-based pharmacophore generation

The active site in Glo-II was used to generate a 3D SBP model to be employed in the virtual screening of small molecules databases. The first 3D pharmacophore was generated using the *Interaction Generation Protocol* available in DS as described in the methods section. The

binding site was defined with a sphere that encompasses all amino acid residues that could contribute to effective ligand binding.

The binding site was analysed by applying the *Interaction Generation* protocol, which uses the Ludi algorithm to generate an interaction map of the binding site. A set of 3D pharmacophoric queries were then derived from the interaction map which were then clustered and edited where the most important features were selected and included in the construction of the primary pharmacophore model (figure 4a).

Replacement of the HBA mapping the Zn atom with a customized Zn-binding feature: Different studies have shown that the presence of Zn-binding groups plays a crucial role in the activity of many inhibitors of zinc metalloproteins such as histone deacetylase inhibitors[30] and matrix metalloproteinase inhibitors[31]. Since Glo-II is a metalloprotein with two Zn ions in its active site, the inclusion of a ZBG feature in the generated 3D pharmacophore is important for effective VS of small molecules DB for potential Glo-II inhibitors. Therefore, the HBA features that mapped the Zn ions in the *Interaction Generation Protocol* were manually replaced by a Zn-binding feature using *Add Feature from Dictionary* under *Customize Pharmacophore Features* tools within DS (figure 4b). The added Zn-binding feature is a modified ZN-BINDER feature in DS which has been previously customised by our group[32]. To this modified feature further customization was carried out by incorporating extra ZBG obtained from the literature that are proved to be effective Zn binders[30, 31, 33] (table 2).

The Receptor-Ligand Pharmacophore Generation protocol: This protocol was utilised to generate two pharmacophores based on the Glo-II GSH and Glo-II GBP complexes as described in the methods section. In this study 10 pharmacophore models were generated for each complex and the top ranked one for each complex was used to build the final pharmacophore. The top ranked model from the Glo-II GBP complex consisted of 6 features: 3HBA, HBD, RA, and NI (figure 5a). The top ranked model from the Glo-II GSH complex consisted of 6 features: 3HBA, 2HBD, and NI (figure 5b).

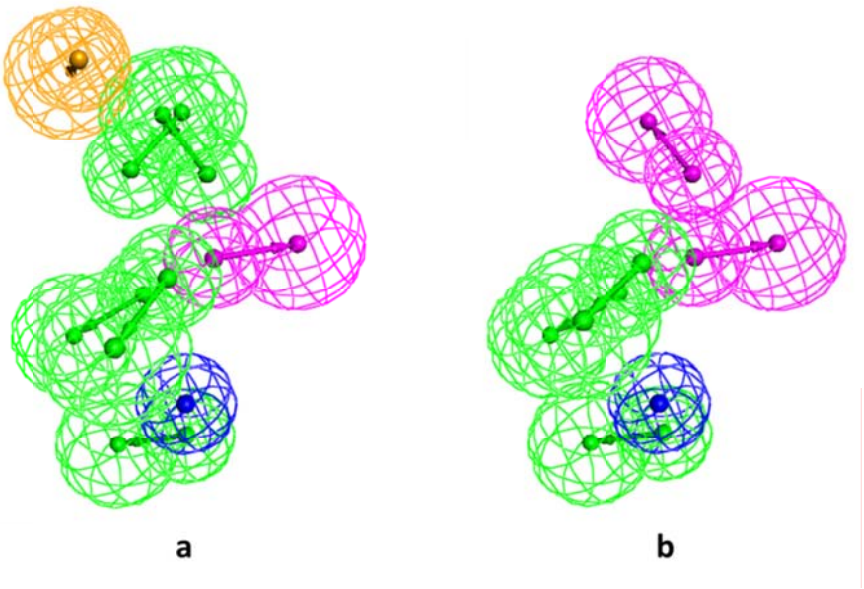

Figure 5: Pharmacophores generated using the *Receptor-Ligand Pharmacophore Generation* protocol, (a) Glo-II GBP complex. (b) Glo-II GSH complex. The feature types in this pharmacophore are: HBD (magenta), HBA (green), ring aromatic (orange), and negative ionisable (blue)

Generation of the final pharmacophore: The final 3D pharmacophore consisted of five features: 2 HBD, HBA, RA, and Zn-binder (figure 6). Functional groups of candidate ligands must map all the pharmacophoric features and reside within the tolerance sphere to be retrieved as hits.

Among the common ZBG is the hydroxamates and the thiol groups. However, hydroxamate group has proved not to be successful in clinical trials due to selectivity, pharmacokinetics and oral bioavailability issues[31, 34]; and the thiols are associated with taste disturbances and photosensitivity in some patients[35, 36]. These two ZBG were removed from the customized Zn-binder feature.

To account for the steric interactions with the target protein, excluded volumes were added to the generated pharmacophore as described in the methods section; these define regions within the binding site that a ligand may not overlap (figure 6a). This makes the search query more specific and excludes ligands that would clash with protein atoms in the binding site.

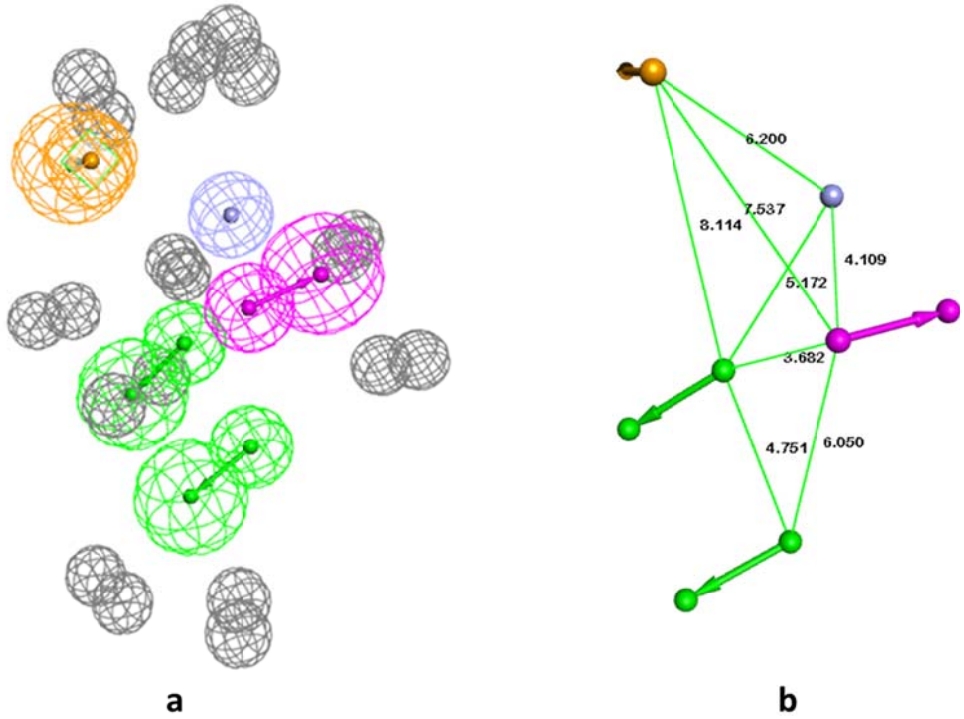

Figure 6: The final structure-based pharmacophore model (a) and the inter-feature distances (b). The feature types in this pharmacophore are: HBD (magenta), HBA (green), Zn-binder (light blue), and excluded volumes (grey)

Usually it is a good practice to validate pharmacophores before using them to screen databases. The validation is performed by using a set of ligands with known binding modes or binding affinities. In this instance, four *N*- and *S*-blocked glutathione derived inhibitors for Glo-II from *Arabidopsis thaliana* (inhibitors 7-10 in table 1) were used to validate the final generated pharmacophore[23]. All four inhibitors mapped the pharmacophore (figure 7). Having validated the generated pharmacophore, virtual screening of small molecules databases commenced.

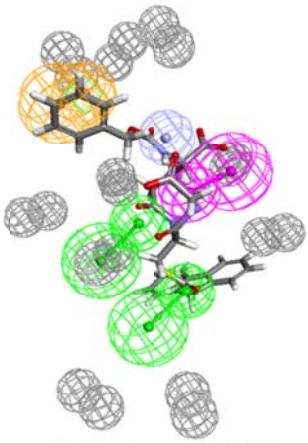

Figure 7: Overlay of inhibitor 10 over the generated pharmacophore

3. Virtual screening of commercial databases

The Maybridge 2013 and NCI 2012 Databases were searched for hits that fit to the generated pharmacophore as described in the methods section. More than 54,000 compounds in Maybridge DB and 265000 in NCI DB were screened and all ligands that mapped the pharmacophore were retained. A total of 5828 hits were retained. 860 hits were retained from screening Maybridge DB, and 4968 hits from NCI. The retrieved hits with the highest fit value from Maybridge and NCI are mapped upon the pharmacophore in figure 8.

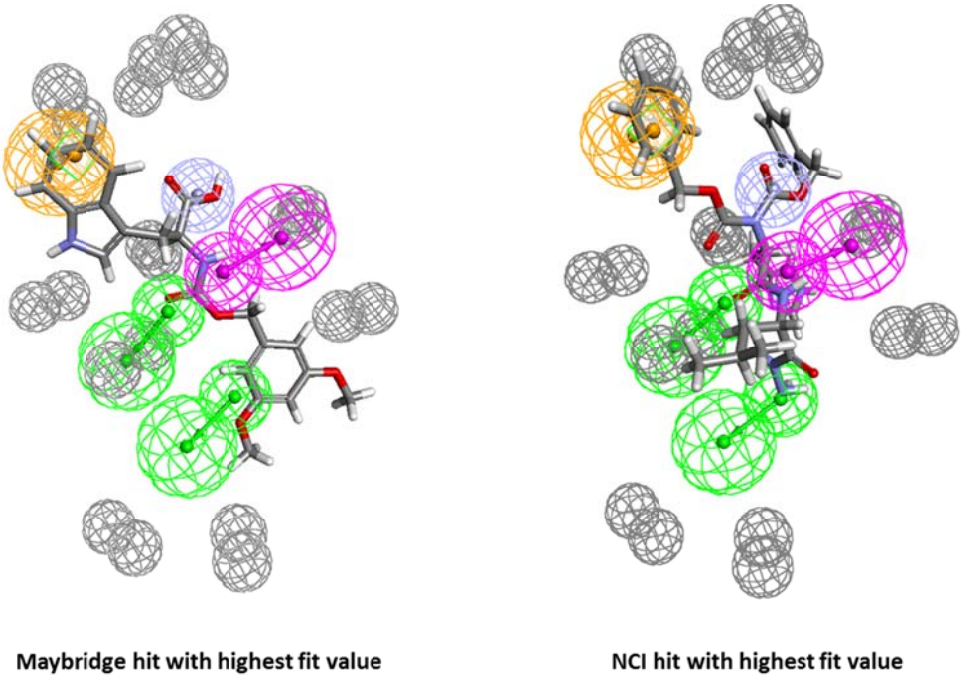

Figure 8: Overlay of retrieved hits with the highest fit value from Maybridge (fit value 3.034) and NCI (fit value 4.15) databases over the pharmacophore

Retrieved hits were filtered based on Lipinski's rule of five for drug like properties. For a compound to obey Lipinski's rule it has to have a molecular weight of less than 500; less than 5 hydrogen-bond donor groups; less than 10 hydrogen-bond acceptor groups; and a partition coefficient (ALogP) of less than 5. Maybridge hits that passed the filtration process were 621, and that of NCI were 2127 (3080 hits have failed) to end up with 2748

hits. Further filtration was conducted based on consideration of the fit values. The threshold for the fit value used to filter the retrieved hits was set to be equal to or more than 2.0. This threshold is an arbitrary one chosen based on the range of the fit values of retrieved hits (Maybridge hits 1.18e-05 to 3.034, and NCI 2.95e-07 to 4.15). In this pharmacophore we have 5 features thereby the highest possible fit value would be 5. But since we incorporated exclusion spheres it is usually unlikely to have such a high fit value. In our case it was chosen to be 50% or above of the highest obtained fit value (4.15). The fit values of the retrieved hits are based on how well the hits map the pharmacophoric features and whether they deviate from the centre of the feature or not; the better the fit, the higher the fit value score.

Maybridge hits that passed the threshold fit value were 68, and that of NCI were 331 (2349 hits failed) to end up with 399 hits. A final filtration step was by applying ADMET filter to exclude hits that might have unfavourable ADMET properties. Out of the 68 Maybridge hits 58 passes the ADMET filter; and 257 of those retained from filtered NCI hits. Hits that passed all filtration criteria were 315 and they were selected for molecular docking. Figure 9 summarises all filtration processes.

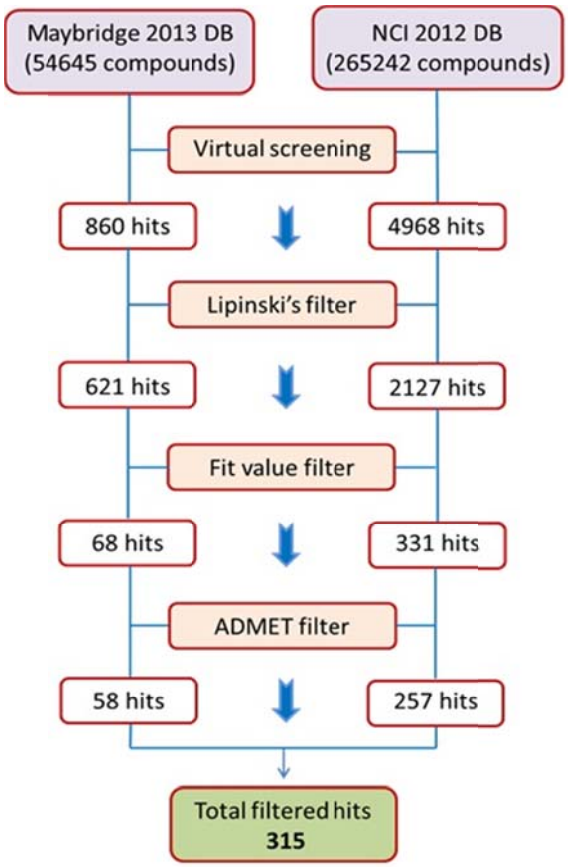

Figure 9: The filtration process of the retrieved hits from VS of Maybridge 2013 and NCI 2012 DBs

4. Molecular Docking and consensus scoring

Molecular docking of the filtered hits was performed using CDOCKER, and GOLD version 5.1. In both docking runs the Glo-II GBP complex was used to define the binding site. The binding site in GOLD and in CDOCKER was defined as described previously.

CDOCKER docking: the 315 filtered hits were docked into the defined binding site of the Glo-II enzyme. The

CDOCKER interaction energy scores for the Maybridge hits were ranging from 29.54 to 59.61 Kcal/mol; and that of the NCI hits were ranging from 27 to 67.5 Kcal/mol. The docked ligands were then rescored using different scoring functions in order to perform a consensus scoring as described in the methods section. The PMF04 scores for the Maybridge hits were ranging from (73.73 - 182.58 Kcal/mol), and the PLP2 scores were (26.11 - 99.41 Kca/mol). The PMF04 scores for the NCI hits were ranging from (69.58 – 184.77 Kcal/mol), and that for the PLP2 were (30.94 – 103.38 Kca/mol).

GOLD docking: the 315 filtered hits were docked into the defined binding site of the Glo-II enzyme. The Gold-CHEMPLP-fitness scores for the Maybridge hits were ranging from 78.84 to 111.87 Kcal/mol; and that of the NCI hits were ranging from 71.68 to 118.5 Kcal/mol.

Consensus scoring: out of the 58 Maybridge hits, only 9 hits had a consensus score of four (among the top ranked 30%) in CDOCKER interaction energy, the PMF04, the PLP2, and the Gold-CHEMPLP-fitness scoring functions. For the 257 NCI hits, only 30 had a consensus scored of four (among the top ranked 30%). The total number of the combined hits that scored high (consensus score of four) in the consensus scoring was 39 hits.

The docked poses of the 39 hits were visually inspected. Those that showed good binding modes and good molecular interactions with the binding site, and having a reasonable chemical structure were selected as potential inhibitors of the Glo-II enzyme. For example, consider the docked pose of the CDOCKER top ranked hit retrieved from Maybrige DB, RJC02225, which also has a consensus score of four (figure 10). The figure shows that the ZBG (carboxylate) is forming one interaction with Zn2, one with Zn1, and one with the bridging water. Also the indole nitrogen forms a hydrogen bond with Asp58; the two oxygens of the carbamate moiety form two hydrogen bonds with Lys143; and one of the methoxy groups forms a hydrogen bond with Lys252. Furthermore, the phenyl ring of the indole forms a π-π interaction with the imidazole ring of His56, and the dimethoxy-substituted phenyl ring forms a π-cation interaction with Lys252. In total this compound forms 10 interactions with the binding site of the Glo-II enzyme which indicates that this compound could have an excellent affinity for the target enzyme.

Out of the 39 hits 10 compounds were selected whose chemical structures are shown in table 3. In table 3, the ZBGs that are involved in Zn chelation are highlighted in red; and the Zn-ZBG interaction maps are also shown. The binding affinities of selected potential inhibitors will be experimentally evaluated.

In conclusion, in this study a hybrid 3D structure-based pharmacophore model was generated based on crystal structures of Glo-II enzyme in complex with a slow substrate and glutathione. The generated pharmacophore contained a customized Zn-binding feature to make it more selective towards Glo-II which is a binuclear Zn-metalloenzyme. More than 300,000 compounds in Maybridge and NCI databases were virtually screened using the generated pharmacophore aiming to find potential none-glutathione-based inhibitors of the target enzyme. The retained hits were extensively filtered using Lipinski's rule of five, consideration of the fit values, and ADMET properties. Filtered hits were docked into the binding site of the Glo-II enzyme in order to have an estimation of their binding affinity. To further refine the number of retained hits, prioritize them, and to account for the shortcomings of individual scoring function, the docked hits were rescored using different scoring functions followed by consensus scoring. Based on consensus scoring and visual inspection of the chemical structures and binding modes of top ranked hits 10 compounds were selected as potential Glo-II inhibitors. The 10 selected hits will be purchased and their biological activity will be assessed *in vitro* against the target enzyme and against different cancer cell lines

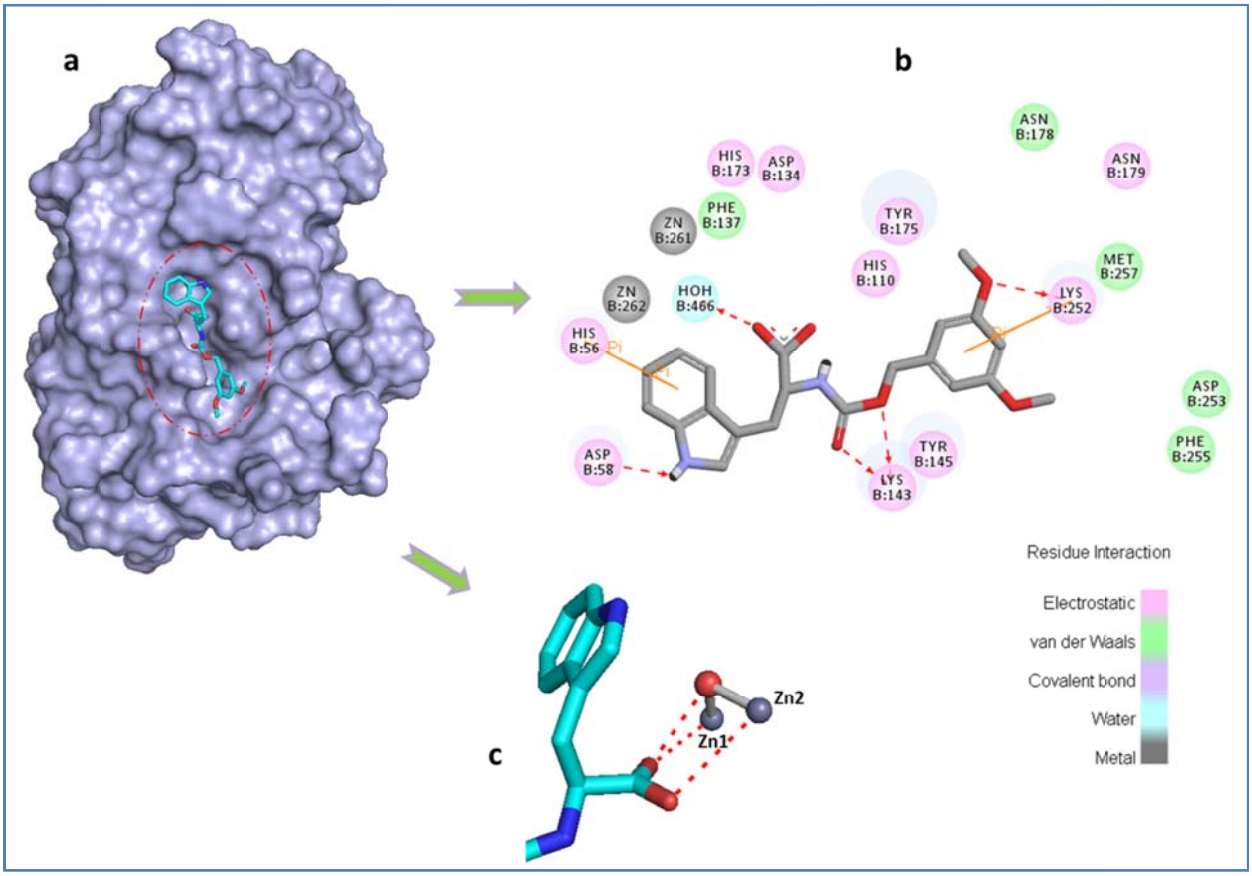

Figure 10: (a) The docked pose of RJC02225 retained from VS of Maybridge DB showing its binding orientation within the binding site of the Glo-II enzyme (dashed red ellipsoid). (b) A 2D interaction map showing the different interactions between the compound and the binding site of the enzyme. Hydrogen bonds with amino acids are shown as dashed red arrows, while pi-pi or cation-pi interactions are in solid orange lines. (c) A close-up view showing the interactions of the carboxylate (ZBG) with Zn ions and the bridging water (dashed green lines)

General Experimental

Computational materials

Preparation of the starting Glo-II structure along with the virtual screening studies were performed using Discovery Studio (DS) 3.5 from BIOVIA® (formerly Accelrys®) Software Inc.[37]. Docking of retrieved hits was performed using CDOCKER[38] within DS, and GOLD from the Cambridge Crystallographic Data Centre (CCDC)[39, 40]. The server hosting DS and GOLD runs 32-bit Microsoft Windows Server 2003 and has four quad core Xeon 2.50 GHz CPUs and 8 Gb RAM. Presentation quality images were generated using the PyMOL Molecular Graphics System[41].

Computational Methods

Preparation of the glyoxalase II enzyme

The structural model of the studied system was prepared for further processing using DS. The initial coordinates for Glo-II were retrieved directly from the Protein Data Bank (entry code 1QH5) which corresponds to Glo-II in complex with Glutathione (GSH) and a substrate analogue S-(N-hydroxy-N-bromophenylcarbamoyl) glutathione (GBP). The PDB

file was checked for missing loops, alternate conformations and incomplete residues using *Protein Report* tool within DS; and none were missing. Then, the structure was cleaned using the *Clean Protein* tool to standardize atoms names, correct connectivity and bond order, and adding hydrogens at a pH of 7.0. Finally, it was typed using the *simulation tools* by applying CHARMm force field.

Structure-based pharmacophore generation

The active site in Glo-II was used to generate a 3D structure-based pharmacophore (SBP) model for the virtual screening of small molecules databases. A SBP utilises known or suspected protein active site to select compounds most likely to bind within that site. The prepared crystal structure of Glo-II was used to generate the pharmacophore by using two approaches, namely; the *Interaction Generation Protocol* and the *Receptor-Ligand Pharmacophore Generation protocol* available in DS.

The Interaction Generation Protocol: This protocol applies the Ludi algorithm to generate the interaction map by numerating interaction points from a protein binding site that are important for ligand binding which are then converted to pharmacophoric features[42, 43]. In order to run the protocol the binding site need to be defined with a sphere that covers all important amino acid residues. The sphere was created using the *Define and Edit Binding Site* tool within DS by defining the enzyme as a receptor then defining the binding sites from the bound ligand. The sphere is then created around the cavity that hosts the bound ligand. The sphere was expanded to 11Å in order to encompass all residues in the binding site that might be of relevance to ligand binding. Having defined the binding site, the protocol was employed, using default parameters, to identify all hydrophobic and hydrophilic interaction points within the sphere that can be complemented by a ligand. The identified hydrogen bond acceptors (HBA), hydrogen bond donors (HBD), and hydrophobic (HY) features were then clustered and edited using the *Edit and Cluster Pharmacophore Features* tool in DS and the most important features were selected and included in the construction of the 3D pharmacophore model.

This protocol treats Zn atoms as hydrogen-bond donors, therefore HBA features complementing the HBD features of the Zn atoms were manually replaced by a Zn-Binder feature. The generated 3D pharmacophore consisted of twelve features (four HBD, four HBA, two HY region and two Zn-binders).

The Receptor-Ligand Pharmacophore Generation protocol: This protocol was utilised to generate two pharmacophores based on the Glo-II GSH and Glo-II GBP complexes. This protocol uses the receptor-ligand complex to generate a set of selective pharmacophore models. A set of pharmacophoric features are identified that correspond to the receptor-ligand interactions. The predefined ligand feature types in DS are: HBD, HBA, HY, negative ionisable (NI), positive ionisable (PI), and ring aromatic (RA). Then, the generated pharmacophore models are enumerated and ranked; the top ranked models were selected. The ranking process is based on measures of selectivity which is predicted from a Genetic Function Approximation (GFA) model[44].

The generation of the final pharmacophore: The final pharmacophore was generated as a hybrid of the above three pharmacophores as follows: all identical features in the three pharmacophores were selected, namely: HBA mapping the amide nitrogen of Lys143; HBA mapping the guanidine moiety of Arg249; and HBD mapping the phenolic OH of Tyr175. In addition, the ring aromatic (RA) feature facing the imidazole moiety of His56 obtained from the receptor-ligand pharmacophore generation protocol of Glo-II GBP complex was included. Finally, a Zn-binder feature from the ones that replaced the HBAs mapping the Zn ions in the interaction generation protocol was included. This feature was placed at the tail of the HBA vector pointing to the Zn2 ion, 2Å from the Zn atom. The distance between the Zn ion in a metalloprotein and the chelating heteroatom proved to be important for effective chelation. Based on Nagata's investigation of the ZBG in protein-ligand complexes obtained from the PDB the median distances between Zn and O, N, and S were found to be 1.99, 2.05, and 2.28 Å, respectively[33].

Accounting for the steric interactions: In order to account for the steric interactions with the target which give rise to false positive hits in virtual screening (ligands that map the pharmacophore but do not show good docking scores because of steric clashes with target), excluded volumes were added to the generated pharmacophore to remove (or minimize) these false positives. All alpha and beta-carbon atoms in residues within 3Å of the pharmacophore query were selected and used to place exclusion constraints around each of them. The exclusion volumes were then edited such that irrelevant excluded volumes were manually removed. The generated final pharmacophore comprises all features deemed important for ligand binding along with 20 exclusion volumes.

Virtual screening of commercial databases

Preparation of the 3D databases: Maybridge screening collection library 2013 with more than 54,000 compounds[45] and NCI 2012 library with more than 265,000 compounds[46] were downloaded. The *Build 3D Database* protocol within DS was employed to generate 3D databases of Maybridge and NCI using the *Best* method for conformation generation, while keeping all other parameters at their default values.

Virtual screening: The generated pharmacophore was used in virtual screening of the prepared databases. DS offers two methods for database searching; the *Fast* rigid and the *Best* flexible methods. In general better results are obtained using the best flexible method. In our study the *Best flexible search* method in the *Search 3D Database* protocol in DS was used. Retained hits were then filtered based on Lipinski's rule of five of drug like properties, consideration of fit values, and ADMET properties. Hits that passed all filtration criteria were selected for molecular docking.

Molecular Docking and consensus scoring

Docking: Molecular docking of the filtered hits was performed using CDOCKER (CHARMm-based DOCKER) within DS, and GOLD (Genetic Optimization for Ligand Docking) docking program version 5.1. CDOCKER is a grid-based molecular dynamics docking algorithm. It treats the protein as a rigid molecule but accounts for full ligand flexibility including bonds, angles, and dihedrals through high temperature molecular dynamics followed by random rotations; and to refine the docked poses it performs a final minimisation or simulated annealing step. The generated poses are then scored based on CHARMm energy (interaction energy plus ligand strain) and the interaction energy alone. The top ranked poses based on interaction energy (the most negative, favourable interaction) are retained[38]. The same sphere-defined binding site used for *Interaction Generation Protocol* was used for docking purposes. Then CDOCKER protocol was employed using default values for all of its parameters.

GOLD uses a genetic algorithm (GA) to perform fully flexible ligand docking with partial flexibility of the binding site[39,47]. GOLD has proved to be one of the most accurate ligand docking programs. Different studies have shown that GOLD was more than 70% (in some cases more than 80%) accurate in reproducing the crystal complex binding mode of the ligand[48, 49]. The Glo-II GBP complex was used to define the binding site. The binding site in GOLD was defined by selecting the ligand and all atoms within 6Å radius of the ligand. The ligand was extracted from the complex and a cavity detection algorithm, LIGSITE, was used to restrict the region of interest to concave, solvent-accessible surfaces. LIGSITE is an automatic program that searches for and detect pockets on protein surfaces that may serve as a binding site for small ligands[50]. Only the top four scored docks out of ten per compound were stored, and early termination was activated. GOLD uses a fitness score to separate and rank all generated conformations of the docked compounds. The Gold fitness score accounts for protein-ligand H-bonding and van der Waal interactions; and ligand's internal van der Waals and torsional strain energy[39]. There are five different scoring functions within Gold; GoldScore, ChemScore, CHEMPLP, ASP, and User defined score.

Consensus scoring: Despite all the advances in the field of molecular docking, developing an accurate and

rapid scoring function to predict the protein-ligand interactions remains the main challenge. However, there are many available scoring functions that can be used in molecular docking studies which can be categorised into three main groups; the force field based scoring functions, the empirical scoring functions, and the knowledge based scoring functions. Each of these classes has its own advantages and drawbacks[51].

In order to optimise docking results and to minimise the possible bias that might be imposed by using a single scoring function is to use consensus scoring. It is a fast way of identifying ligands that score high in more than one scoring function. To calculate a consensus score for a set of docked ligands they need to be rescored by other scoring functions prior to consensus scoring. For each scoring functions, ligands will be sorted in decreasing order of their score. The consensus score for a compound is an integer that is equal to its frequency in the top rank percentile (defined by user) for each scoring function.

In this study, we calculated a consensus score for each of the docked ligands. Firstly, we rescored the docked ligands using different scoring functions available in DS; namely: PMF04 (a knowledge based scoring function), and PLP2 (an empirical scoring function). This was carried out using the *Score Ligand Poses* protocol in DS. Then, a consensus score based on a consensus percentage of 30 was calculated using the *Consensus Score* protocol in DS. Furthermore, a second consensus was performed by comparing hits retained from the first consensus with the top 30% hits retained from Gold docking using the CHEMPLP scoring function (an empirical scoring function).

ACKNOWLEDGMENT

The authors would like to thank the deanship of scientific research at Jordan University of Science and Technology for funding this project.

Table 1. known inhibitors of Glo-II

Index	Chemical structure and name	Inhibits	IC_{50} or Ki	Ref
1	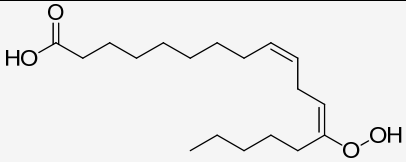 13-Hydroperoxylinoleic acid	Rat liver Glo-II	IC_{50} is below 0.1 µg/ml	[17]
2	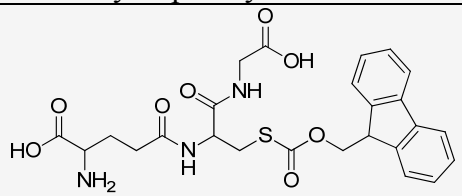 S-(9-fluorenylmethoxycarbonyl)glutathione	Calf liver Glo-II	Ki = 2.1 µmol/l	[18]
3	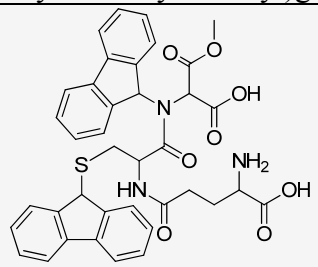 N,S-bis-fluorenylmethoxycarbonylglutathione	Calf liver Glo-II	Ki= 0.08 µM	[19]

4	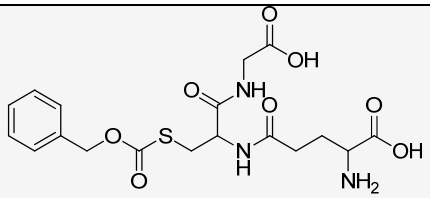 S-carbobenzoxyglutathione	Glo-II from Liver extracts of rat, mouse, and sheep	Ki = 0.065 mM	[20]
5	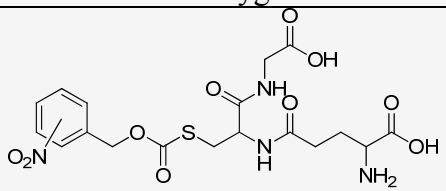 S-(Nitrocarbobenzoxy)glutathiones	Rat liver Glo-II	Ki = 65 µM	[21]
6	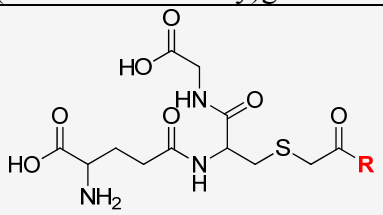 (R) is a hydrophobic moiety such as: C6H5, 3-CH3O-C6H4, 4-CH3O-C6H4, 4-Br-C6H4, C10H7, 4-C6H4-C6H4. Non-hydrolyzing derivatives of S-D-lactoylglutathione with S-site modified	Bovine liver Glo-II	IC_{50} is ranging from 142-276 µM	[22]
7	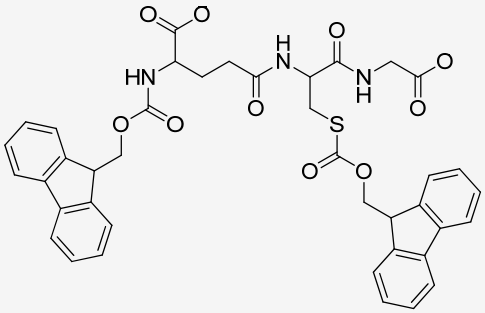 N,S-bis-(9-fluorenylmethoxycarbonyl)glutathione	Arabidopsis thaliana Glo-II	Ki = 0.89 µM	[23]
8	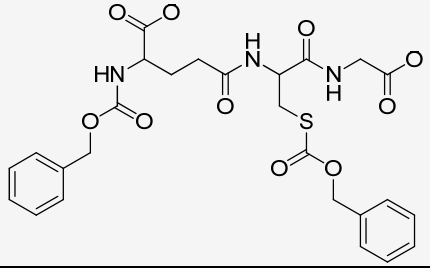	Arabidopsis thaliana Glo-II	Ki = 2.3 µM	[23]

	N,S-bis-phenylmethoxycarbonylglutathione			
9	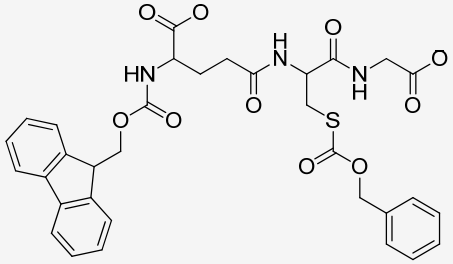 N-(9-fluorenylmethoxycarbonyl)-S-phenylmethoxycarbonyl glutathione	Arabidopsis thaliana Glo-II	Ki = 1.7 μM	[23]
10	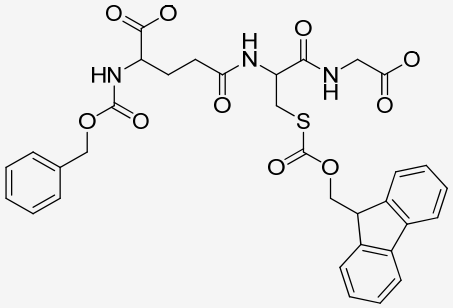 N-phenylmethoxycarbonyl-S-fluorenylmethoxycarbonyl glutathione	Arabidopsis thaliana Glo-II	Ki = 2.0 μM	[23]

Table 2: The extra ZBG incorporated in the customised Zn-binder feature of DS

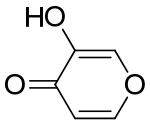	Hydroxypyrone	[31]
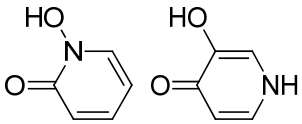	Hydroxypyridinones	[31]
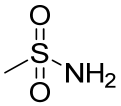	Sulfonamide	[33]
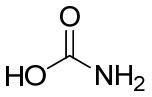	Carbamates	[33]
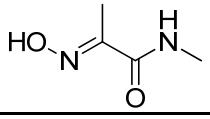	Oxime amide	[30]

Table 3. Selected hits as potential inhibitors of the Glo-II enzyme. ZBGs within the chemical structures are shown in red

1	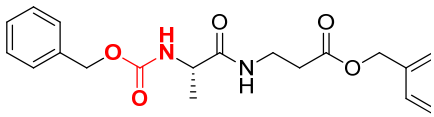 (NCI) 164064	2.71	63.5	174.1	95.7	103.8	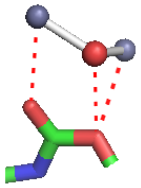
2	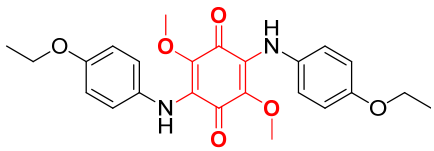 (NCI) 103407	2.75	57.7	167.0	96.8	114.1	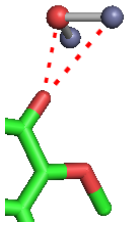
3	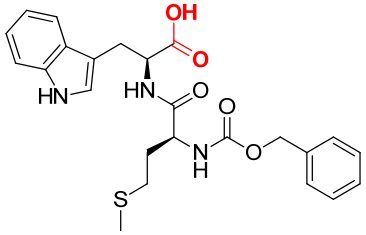 (NCI) 333767	2.57	54.5	184.8	93.9	109.8	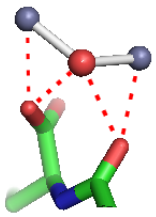
4	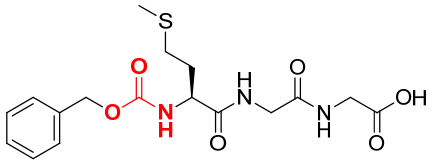 (NCI) 333764	2.56	63.7	172.6	97.6	104.8	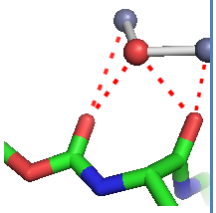
5	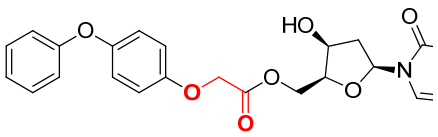 (NCI) 160910	2.49	55.9	180.8	103.4	114.5	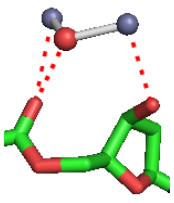

6	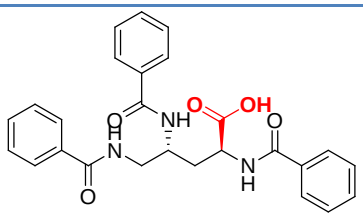 (NCI) 281044	2.31	56.1	161.7	101.5	112.9	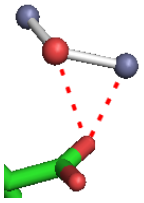
7	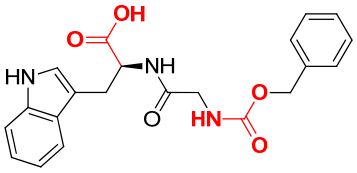 (NCI) 89647	2.36	56.1	182.7	88.9	109.3	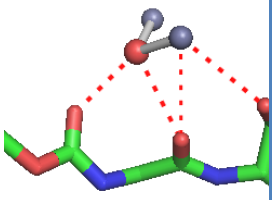
8	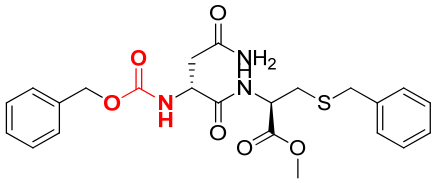 (NCI) 302663	2.00	56.5	170.1	92.2	103.6	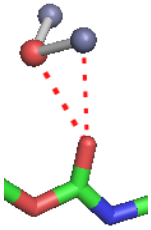
9	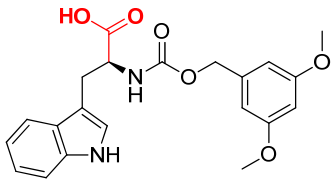 (MB) RJC02225	3.03	54.90	176.8	89.6	108.4	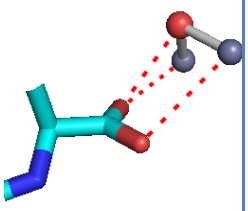
10	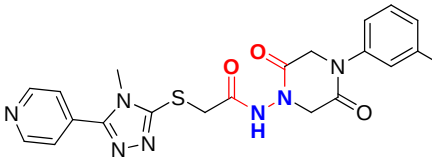 (MB) HTS13268	2.47	59.6	174.8	89.4	104	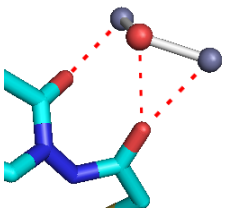

* CDIE, is the CDOCKER interaction energy.

REFERENCES

(1) Thornalley, P.J., *The glyoxalase system: new developments towards functional characterization of a metabolic pathway fundamental to biological life.* ***Biochemical Journal***, 1990. 269:1-11.

(2) Sousa Silva, M. et al., ***The glyoxalase pathway: the first hundred years… and beyond***. ***Biochemical Journal***, 2013. 453 (1): 1-15.

(3) Xue, M., Rabbani, N. and Thornalley, P.J. ***Glyoxalase in ageing***. Seminars in Cell & Developmental Biology, 2011. 22 (3): 293-301.

(4) Phillips, S.A. and Thornalley, P.J. ***The formation of methylglyoxal from triose phosphates***. ***European Journal of Biochemistry***, 1993. 212 (1): 101-105.

(5) Reichard, G.A. et al., ***Acetone Metabolism in Humans During Diabetic Ketoacidosis***. Diabetes, 1986. 35(6): 668-674.

(6) Lyles, G.A. and Chalmers, J. *The metabolism of aminoacetone to methylglyoxal by semicarbazide-sensitive amine oxidase in human umbilical artery.* ***Biochemical Pharmacology***, 1992. 43 (7): 1409-1414.

(7) Vander Jagt, D.L. and Hunsaker, L.A. ***Methylglyoxal metabolism and diabetic complications: roles of aldose reductase, glyoxalase-I, betaine aldehyde dehydrogenase and 2-oxoaldehyde dehydrogenase***. Chemico-Biological Interactions, 2003. 143–144: 341-351.

(8) Thornalley, P.J., Langborg, A. and Minhas, H.S. *Formation of glyoxal, methylglyoxal and 3-deoxyglucosone in the glycation of proteins by glucose.* ***Biochemical Journal***, 1999. 344 (1): 109-116.

(9) Rulli, A., et al., *Expression of glyoxalase I and II in normal and breast cancer tissues.* ***Breast Cancer Research and Treatment***, 2001. 66 (1): 67-72.

(10) Clelland, J.D., Allen, R.E. and Thornalley, P.J. *Inhibition of growth of human leukaemia 60 cells by S-2-hydroxyacylglutathiones and monoethyl ester derivatives.* ***Biochemical Pharmacology***, 1992. 44 (10): 1953-1959.

(11) Edwards, L.G., A. Adesida, and P.J. Thornalley, *Inhibition of human leukaemia 60 cell growth by S-d-lactoylglutathione in vitro. Mediation by metabolism to N-d-lactoylcysteine and induction of apoptosis.* ***Leukemia Research***, 1996. 20 (1): 17-26.

(12) Edwards, L.G. and P.J. Thornalley, *Prevention of S-d-lactoylglutathione-induced inhibition of human leukaemia 60 cell growth by uridine.* ***Leukemia Research***, 1994. 18(9): 717-722.

(13) Thornalley, P.J. and M.J. Tisdale, *Inhibition of proliferation of human promyelocytic leukaemia HL60 cells by S-d-lactoylglutathione in vitro.* ***Leukemia Research***, 1988. 12 (11–12): 897-904.

(14) Mearini, E. et al., *Differing expression of enzymes of the glyoxalase system in superficial and invasive bladder carcinomas.* ***European Journal of Cancer***. 38 (14): 1946-1950.

(15) Vince, R., S. Daluge, and W.B. Wadd, *Inhibition of glyoxalase I by S-substituted glutathiones.* ***Journal of Medicinal Chemistry***, 1971. 14 (5): 402-404.

(16) Creighton, D.J. et al., *Glyoxalase I inhibitors in cancer chemotherapy.* Biochemical Society Transactions, 2003. 31 (part 6): 1378-1382.

(17) Gillespie, E., *13-Hydroperoxylinoleic acid inhibits rat liver glyoxalase II.* Inflammation (N.Y.), 1981. 5 (Copyright (C) 2014 American Chemical Society (ACS). All Rights Reserved.): 203-11.

(18) Chyan, M.K., et al., *S-fluorenylmethoxycarbonyl glutathione and diesters: inhibition of mammalian glyoxalase II.* Enzyme Protein, 1995. 48 (Copyright (C) 2014 American Chemical Society (ACS). All Rights Reserved.): 164-73.

(19) Elia, A.C., et al., *N,S-bis-fluorenylmethoxycarbonyl glutathione: A new, very potent inhibitor of mammalian glyoxalase II.* Biochem. Mol. Biol. Int., 1995. 35 (Copyright (C) 2014 American Chemical Society (ACS). All Rights Reserved.): 763-71.

(20) Hsu, Y.R. and Norton, S.J. *S-Carbobenzoxyglutathione: a competitive inhibitor of mammalian glyoxalase II.* ***J. Med. Chem***., 1983. 26 (Copyright (C) 2014 American Chemical Society (ACS). All Rights Reserved.): 1784-5.

(21) Bush, P.E. and Norton, S.J. *S-*

(Nitrocarbobenzoxy)glutathiones: potent competitive inhibitors of mammalian glyoxalase II. J. Med. Chem., 1985. 28 (Copyright (C) 2014 American Chemical Society (ACS). All Rights Reserved.): 828-30.

(22) Shin, S.S., Lim, D.and Lee, K. *Designing on non-hydrolyzing derivatives for G1xII inhibitors: Importance of hydrophobic moiety in S-site.* Bull. Korean Chem. Soc., 2003. 24 (Copyright (C) 2014 American Chemical Society (ACS). All Rights Reserved.): 897-898.

(23) Yang, K.W. et al., *Explaining the inhibition of glyoxalase II by 9-fluorenylmethoxycarbonyl-protected glutathione derivatives.* ***Archives of Biochemistry and Biophysics***, 2003. 414 (2): 271-278.

(24) Cameron, A.D. et al., *Crystal structure of human glyoxalase I—evidence for gene duplication and 3D domain swapping.* ***The EMBO Journal***, 1997. 16(12): 3386-3395.

(25) Cameron, A.D. et al., *Crystal structure of human glyoxalase II and its complex with a glutathione thiolester substrate analogue.* ***Structure***, 1999. (9): 1067-1078.

(26) Zang, T.M. et al., *Arabidopsis Glyoxalase II Contains a Zinc/Iron Binuclear Metal Center That Is Essential for Substrate Binding and Catalysis.* ***Journal of Biological Chemistry***, 2001. 276 (7): 4788-4795.

(27) Berman, H.M. et al., *The Protein Data Bank.* Acta Crystallographica Section D, 2002. 58 (6 Part 1): 899-907.

(28) Campos-Bermudez, V.A. et al., *Metal-dependent inhibition of glyoxalase II: A possible mechanism to regulate the enzyme activity.* ***Journal of Inorganic Biochemistry***, 2010. 104 (7): 726-731.

(29) Chen, S.L., Fang, W.H. and Himo, F. *Reaction mechanism of the binuclear zinc enzyme glyoxalase II – A theoretical study.* ***Journal of Inorganic Biochemistry***, 2009. 103 (2): 274-281.

(30) Botta, C.B. et al., *Oxime Amides as a Novel Zinc Binding Group in Histone Deacetylase Inhibitors: Synthesis, Biological Activity, and Computational Evaluation.* ***Journal of Medicinal Chemistry***, 2011. 54 (7): 2165-2182.

(31) Agrawal, A. et al., *Zinc-Binding Groups Modulate Selective Inhibition of MMPs.* ChemMedChem, 2008. 3 (5): 812-820.

(32) Al-Balas, Q. et al., *Generation of the First Structure-Based Pharmacophore Model Containing a Selective "Zinc Binding Group" Feature to Identify Potential Glyoxalase-1 Inhibitors.* ***Molecules***, 2012. 17 (12): 13740-13758.

(33) Kawai, K. and Nagata, N. *Metal–ligand interactions: An analysis of zinc binding groups using the Protein Data Bank.* ***European Journal of Medicinal Chemistry***, 2012. 51 (0): 271-276.

(34) Govinda B.R., *Recent Developments in the Design of Specific Matrix Metalloproteinase Inhibitors aided by Structural and Computational Studies.* ***Current Pharmaceutical Design***, 2005. 11 (3): 295-322.

(35) Scully, C. and Bagan, J. V. *Adverse Drug Reactions in the Orofacial Region.* ***Critical Reviews in Oral Biology & Medicine***, 2004. 15 (4): 221-239.

(36) Douglass, R. and Heckman, G. *Drug-related taste disturbance.* Canadian Family Physician, 2010. 56.

(37) *Discovery Studio*. 2013, Accelrys Inc.: San Diego, CA, USA.

(38) Wu, G. et al., *Detailed analysis of grid-based molecular docking: A case study of CDOCKER—A CHARMm-based MD docking algorithm.* ***Journal of Computational Chemistry***, 2003. 24 (13): 1549-1562.

(39) Verdonk, M.L. et al., *Improved protein-ligand docking using GOLD.* Proteins-Structure Function and Genetics, 2003. 52 (4): 609-623.

(40) Krusek, J. *Allostery and Cooperativity in the Interaction of Drugs with Ionic Channel Receptors.* ***Physiological Research***, 2004. 53: 569-579.

(41) Michael D. Daily and Jeffrey J. Gray, *Allosteric Communication Occurs via Networks of Tertiary and Quaternary Motions in Proteins.* ***PLoS Computational Biology***, 2009. 5 (2).

(42) Böhm, H.J., *LUDI: rule-based automatic design of*

new substituents for enzyme inhibitor leads. ***Journal of Computer-Aided Molecular Design***, 1992. 6 (6): 593-606.

(43) Böhm, H.J., *The computer program LUDI: A new method for the de novo design of enzyme inhibitors.* ***Journal of Computer-Aided Molecular Design***, 1992. 6 (1): 61-78.

(44) Rogers, D. and Hopfinger, A.J. *Application of Genetic Function Approximation to Quantitative Structure-Activity Relationships and Quantitative Structure-Property Relationships.* ***Journal of Chemical Information and Computer Sciences***, 1994. 34 (4): 854-866.

(45) Erbeck, A. and Brush, E.J. *Synthesis of indole and oxindole derivatives of glutathione as potential inhibitors of glyoxalase II*. 2006: American Chemical Society.

(46) *NCI Database*. 2012; Release 4 File Series-May 2012: [Available from: http://cactus.nci.nih.gov/.

(47) Jones, G. et al., *Development and validation of a genetic algorithm for flexible docking.* ***Journal of Molecular Biology***, 1997. 267(3): 727-748.

(48) Hartshorn, M.J. et al., *Diverse, High-Quality Test Set for the Validation of Protein−Ligand Docking Performance.* ***Journal of Medicinal Chemistry***, 2007. 50 (4): 726-741.

(49) Nissink, J.W.M. et al., *A new test set for validating predictions of protein–ligand interaction.* Proteins: ***Structure, Function, and Bioinformatics***, 2002. 49 (4): 457-471.

(50) Hendlich, M., Rippmann, F. and Barnickel, G. *LIGSITE: automatic and efficient detection of potential small molecule-binding sites in proteins.* ***Journal of Molecular Graphics and Modelling***, 1997. 15 (6): 359-363.

(51) Sheng-You, H., Z.G. Sam, and Xiaoqin, Z. *Scoring functions and their evaluation methods for protein–ligand docking: recent advances and future directions*. ***Physical Chemistry Chemical Physics***, 2010. 12: 12899-12908.

تحديد مثبطات محتملة لانزيم الغليوكساليز-٢. كأدوية مضادة للسرطان باستخدام حامل للخاصية الدوائية مخصص ثلاثي الأبعاد

نزار الشرع[١*]، محمد حسان[١]، قصي البلص[١]، عمار المعايطة[٢]

[١] قسم الكيمياء الطبية والعقاقير، كلية الصيدلة، جامعة العلوم والتكنولوجيا الأردنية، الأردن.

[٢] قسم الصيدلة التكنولوجية، كلية الصيدلة، جامعة العلوم والتكنولوجيا الأردنية، الأردن.

ملخص

نظام الغليوكساليز (الذي يتكون من إنزيمي غليوكساليز ١ و٢) هو مسار أيضي موجود في العصارة الخلوية لكل الخلايا وبعض العضيات الأخرى داخل الخلية. وتكمن أهميته في إزالة السمية الخلوية لمركبات الاكسوالديهاد (oxoaldehydes)، ولا سيما الميثل غليوكسال (methylglyoxal) ومنتجه الأيضي اللاكتويل غلوتاثيون (S-D-lactoylglutathione)، وتحويلها إلى مركبات غير سامة من مشتقات حمض هيدروكسي الكاربوكسيل (2-hydroxycarboxylic acid). يكون النشاط الأيضي في الخلايا السرطانية أعلى منه في الخلايا الطبيعية حيث يؤدي إلى زيادة مستويات هذه السموم الأيضية داخل الخلايا، مما يحفز الخلايا السرطانية على زيادة نشاط هذه الإنزيمات لتقليل تركيز هذه المركبات داخل الخلايا، وإزالة سميتها بطريقة متوازنة مما يجعل هذين الانزيمين هدفا لتطوير عقاقير مضادة للسرطان.

في هذه الدراسة، تم تصميم نموذج لحامل الخاصية الدوائية (pharmacophore) ثلاثي الأبعاد اعتماداً على التركيب البلوري لإنزيم الغليوكساليز-٢ المرتبط بمركب مشابه للمركب الطبيعي لهذا الإنزيم. هذا النموذج هو هجين من ثلاثة نماذج ثلاثية الأبعاد. وبما أن إنزيم الغليوكساليز-٢ هو إنزيم فلزي حيث يحتوي علي ذرتي زنك، فقد تم إضافة مجموعة مميزة للزنك في هذا النموذج للمساعدة في البحث عن مركبات ذات قدرة انتقائية على تثبيط عمل هذا الإنزيم من خلال البحث الافتراضي في قواعد البيانات للمركبات صغير الحجم، وهما قاعدة بيانات ميبردج (Maybridge) وان سي اي (NCI)، حيث تحتويان أكثر من ثلاثة مائة ألف ٣٠٠٠٠٠ مركب. تم تصفية هذه المركبات استنادا إلى قاعدة ليبينسكي الخماسية، وملامة المركب للنموذج، وخصائص المركب من حيث الامتصاص والتوزيع والأيض والطرح والسمية (ADMET properties). من ثم تم دراسة كيفية ارتباط المركبات التي اجتازت عملية التصفية بموقع الارتباط من الإنزيم باستخدام اثنين من الخوارزميات وهما جولد (GOLD) وسي دوكر (CDOCKER) وإعطاء قيمة تقريبية لمقدار الطاقة الناتجة عن ارتباط المركب بالإنزيم. ومن أجل تحقيق أقصى قدر من فرص العثور على مثبطات محتملة لهذا الانزيم، تم اعادة تقييم مقدار طاقة الارتباط لهذه المركبات باستخدام معادلات تقييم أخرى وحساب القيمة الكلية لجميع معدلات التقييم من أجل اختيار المركبات ذات المجموع الأكبر. من هذه المركبات، أعلى عشرة مركبات تم اختيارهم كمثبطات محتملة للإنزيم.

الكلمات الدالة: إنزيم الغليوكساليز، السرطان، فحص ثلاثي الأبعاد.

تاريخ استلام البحث ٢٠١٤/١/٤ وتاريخ قبوله للنشر ٢٠١٥/٤/٤.